Industrial Crops & Products 181 (2022) 114833

Contents lists available at ScienceDirect

Industrial Crops & Products

journal homepage: www.elsevier.com/locate/indcrop

# Authentication of Styrax officinalis L. methyl ester nanoparticulate fuel-system's suitability in powering CI engines

Babalola Aisosa Oni [a,*], Samuel Eshorame Sanni [b], Anayo Jerome Ibegbu [c], Tomiwa Isaac Oguntade [d]

[a] Chemical Engineering Department, China University of Petroleum, Changping District, Beijing City, PR China
[b] Department of Chemical Engineering, Covenant University, P.M.B 1023, Ota, Nigeria
[c] Department of Mechanical Engineering, Madonna University, Elele, Nigeria
[d] Department of Petroleum Engineering, University of North Dakota, Grand Forks, North Dakota, USA

ARTICLE INFO

*Keywords:*
Styrax officinalis L. biodiesel
Nanoparticles
Emissions
Diesel engine
Nanoparticle stability
Brake thermal efficiency

ABSTRACT

Investigation was carried out on the engine performance, combustion and emission characteristics of a CI engine using biodiesel-nanoparticulate fuel-system formulated using ultrasonicated cerium, aluminum and titanium oxide nanoparticles mixed with Styrax officinalis L. seed oil methyl esters. The nanofluids were prepared using 75, 58, and 83 ppm of aluminum, titanium, cerium dioxides. The physicochemical characteristics of the nano-fuels were determined and compared with those of conventional diesel in a Lister petter engine under various engine loads. The stabilities of the nanoparticles were analyzed under static conditions. There was marginal enhancement in the engine performance where the brake thermal efficiencies (BTEs) of the biodiesel doped with 75 ppm $Al_2O_3$ (S-C), 58 ppm $TiO_2$ (S-D), and 83 ppm $CeO_2$ (S-E) nanoparticles were 34.1%, 37.1% and 35.9% compared to those of the neat biodiesel and conventional diesel which were 31.2% and 31.9% respectively. Furthermore, the HC, $NO_x$ and CO emissions of the nano-fuel decreased at full load. Combustion properties of the in-cylinder pressure and the heat release rate improved upon the addition of the nanoparticles to the biodiesel. Therefore, the nano-fuels improved the engine's performance and can satisfactorily be used as fuel in an unmodified diesel engine.

## 1. Introduction

The persistent rise in the world's population and the widespread use of fossil fuels has led to the need for a sustainable eco-friendly energy source as alternative fuel (Oni and Oluwatosin, 2020; Oni et al., 2021b; Simsek and Uslu, 2020). At the moment, fossil-based energy sources meet 80% of the world's energy demand. However, the major challenges with the use of diesel from fossil fuel are environmental degradation (emissions from greenhouse gases) and public health concerns (air pollution) (Oni et al., 2021c, 2021d).

Clean-burning renewable fuels are fast becoming dependable alternatives to conventional diesel due to the ease with which they can be synthesized (Oni et al., 2021e). Besides the use of diesel from fossil-fuel, several studies have focused on alternative biofuels for use in compression ignition engines, with the goal of improving engine performance with low exhaust emissions (Oni et al., 2021d, 2021e).

Biofuel is considered as an eco-friendly renewable fuel that releases less amount of smoke, unburned HCs and CO compared to conventional diesel fuel (Oni and Oluwatosin, 2020). Compared to conventional diesel, biodiesel's molecular structure contains additional oxygen atoms, which contribute more oxygen that aids combustion. Despite their numerous advantages, biofuels have several downsides, such as high viscosity, poor cold flow qualities and poor heating values (Simsek and Uslu, 2020). Several biodiesel properties have been reported in literature; they include those of Jojoba oil (Oni and Oluwatosin, 2020), neem oil, Jatropha oil, Moringa oleifera *oil,* Cerbera odollam oil and Camelina oil, which were also tested for use in diesel engines (Oni et al., 2021b; Simsek and Uslu, 2020). These crude vegetable oils typically produced higher emissions, which has made recent biofuel researches to focus on searching suitable additives for biodiesel which will not only enhance engine performance but in turn lower emissions (Simsek and Uslu, 2020).

Biorefining is one of the circular economy's core enablers, thus

* Corresponding author.
*E-mail addresses:* babalola.oni@covenantuniversity.edu.ng (B.A. Oni), samuel.sanni@covenantuniversity.edu.ng (S.E. Sanni), anayo.jerome@yahoo.com (A.J. Ibegbu), tomiwa.oguntade@und.edu (T.I. Oguntade).

https://doi.org/10.1016/j.indcrop.2022.114833
Received 13 December 2021; Received in revised form 16 February 2022; Accepted 21 March 2022
Available online 28 March 2022
0926-6690/

**Nomenclature**

| | |
|---|---|
| $NO_x$ | Nitrogen oxide |
| HRR | Heat release rate |
| SDS | Sodium dodecyl sulfate |
| BTE | Brake thermal energy |
| CO | Carbon monoxide |
| HC | Hydrocarbons |
| ID | Ignition delay |
| CI | Compression ignition |
| SEM | Scanning electron microscopy |
| $CeO_2$ | Cerium Oxide |
| $TiO_2$ | Titanium oxide |
| $Al_2O_3$ | Aluminum Oxide |
| CR | Compression ratio |
| CP | In- Cylinder pressure |
| NPs | Nanoparticles |
| BSEC | Brake specific energy consumption |

closing the loops encountered with the use of raw biomass materials (industry, forestry reuse, agriculture and post-consumer leftovers), carbon, minerals, and water. As a result, biorefining is the best technique for large-scale, long-term biomass use in the bio-economy (Morone and Yilan, 2020). It will result in cost-competitive co-production of food/-feed components, bio-based products, and bio-energy with the best socio-economic and environmental outcomes (efficient use of resources, reduced greenhouse gas emissions, etc.). The bio-refinery economy envisions a future in which bio-renewables take the place of fossil fuels (Gebremariam and Marchett, 2018). The move to a biorefinery economy will necessitate significant additional infrastructure investment to produce, store, and deliver biorefined goods to end customers. Better energy security, decreased environmental effect, foreign exchange earnings, and socio-economic difficulties relating to the rural sector are all advantages of biofuels over fossil fuels. Biofuel technology is also valuable to both emerging and developed nations (IEA, 2015). As a result of these factors, biofuels are likely to increase quickly in the vehicle fuel market within the next decade. Increased income taxes, sustainability, increasing number of rural manufacturing jobs, international competitiveness, fuel diversity, greater expenditures in plant and equipment, agricultural development, international competitiveness, and reduced dependence on imported petroleum products are some of the potential/economic benefits of biofuels (Morone and Yilan, 2020; IEA, 2015). Consequently, biodegradability, GHG reductions, air pollution reductions, increased combustion efficiency, improved land and water utilization, and carbon sequestration are also environmental benefits of biofuels (Hasan and Rahman, 2017).

Yesilyurt and Cesur (2017) conducted an experiment on the use of Styrax officinalis L. seed-oil biodiesel; the fuel properties were within the range of the EN 14214 specifications. The authors concluded that the biodiesel can be used as a suitable feedstock for the production of biodiesel.

Till date, not much work has been carried out on the use of Styrax officinalis L. seed-oil methyl ester as fuel with the intent of monitoring combustion, emission, and performance characteristics of the fuel in a CI engine.

Styrax officinalis L. is a plant that grows in the Mediterranean and Mid Black Sea regions of Turkey Tropical sections of America and some parts of Southeast Asia. It is a perennial shrub oilseed plant (Moser, 2016) with relatively high oil seed content (about 50%), which implies that if cultivated, the plant can give substantial economic and ecological benefits. In terms of industrial value, this plant is important, because it can grow in non-agricultural environments, desolate, deteriorated surfaces and woodlands (Yesilyurt and Cesur, 2017; Chuah et al., 2016). Furthermore, it has several characteristics that are appropriate for exploring the notions of climate change and global warming (Pinzi et al., 2009) as a new plant under new climatic conditions which is barely given adequate consideration. The use of oil from seeds as an energy source in industrial applications can help reduce the demand for culinary oils. At the same time, the oil has the potential to contribute to the global food security (Simsek and Uslu, 2020; Oni et al., 2021e; Gebremariam and Marchett, 2018). According to Yesilyurt and Cesur (2017), about 3870.00 kg of this seed oil can be obtained from one hectare of arable land which is the average oil yield of many plants.

High viscosity and NOx, low cetane number, cold weather conditions, and frequent maintenance of engine components, lines, fuel tanks, clogged fuel filters, and low brake thermal efficiency are among the limitations inherent in the use of pure biodiesel in diesel engines (Soudagar et al., 2018). Nanoparticle inclusion as an additive to biodiesel fuel optimizes the qualities of neat biodiesel.

Currently, a process for improving the qualities of the fuel by adding fuel additives has been established (Oni et al., 2021e). Over the last decade, the usage of alcohol-based additive in biofuel blend has expanded, thus providing additional oxygen in the combustion chamber which lowers the resulting emissions. In addition, the development of a lean mixture, reduces the biofuel's calorific value which when combined with greater auto ignition temperatures and poorer lubricating properties, leads to a reduction in engine-performance characteristics and increased potential for damage (Gowtham and Prakash, 2020; Paramashivaiah et al., 2018; Agbulut et al., 2020). As a result, scientists have looked into the possibility of nanoparticle additions to improve biofuel qualities.

In reference to the recent advances in the use of fuel additives to alter biodiesel properties, nanotechnology is a potential technology for achieving this great stride alongside achieving good fuel-quality, enhanced engine performance as well as reduced exhaust emissions with improved combustion properties (Soudagar et al. 2018; Paramashivaiah et al., 2018).

Some studies have reported that adding nanoparticles to biodiesel improves the performance of the engine as well as the combustion characteristics with low exhaust emissions (NOx, CO, $CO_2$, HC and $SO_2$) (Ettefaghi et al., 2018; Dubey et al., 2019; Dogana et al., 2020; Oni et al., 2021a; Basha and Anand, 2011).

Although, several works have been carried out on the use of nanoparticle addition on the adoption of several biodiesel fuels such as Calophyllum Innophyllum, Polanga oil, jatropha, *Oenothera lamarckiana*, jojoba, Juliflora, Pongamia methyl esters etc., as fuels in diesel engines, however, no works have reported the use of titanium, alumina and cerium as additives in Styrax officinalis L. seed oil biodiesel with an optimum concentration that will result in higher engine performance, better combustion and minimal emissions in an unmodified compression ignition engine. Hence, this study aims at ascertaining the optimum conditions for the use of $Al_2O_3$, $TiO_2$, and $CeO_2$ nanoparticles admixed with Styrax officinalis L. biodiesel in CI engine towards achieving improved engine performance, low emissions and better combustion characteristics.

## 2. Materials and method

### *2.1. Extraction of crude oil and production of Styrax officinalis L. methyl esters*

Styrax officinalis L seeds were screw pressed to produce one liter of oil. Thereafter, heat was applied at a temperature of 55 °C. The catalyst was prepared in a 1:30 (weight: volume) ratio of $CH_3OH$ + NaOH; the solution was allowed to mix for about 25 min to produce sodium methoxide. Using a magnetic stirrer, the prepared catalyst was slowly added to the filtered and heated oil at a temperature of 55 °C for 25 min. The mixture was allowed to settle for 20 h in order to allow for the complete separation of glycerol and biodiesel. The biodiesel was then

**Table 1**
Fuel types and nanoparticle additives

| S/N | Biodiesel/ diesel fuel | Concentration of nanoparticle in ppm added to biodiesel. | Acronyms |
|---|---|---|---|
| 1 | Diesel fuel (D100) | – | D-100 |
| 2 | Styrax officinalis L. seeds oil methyl esters (B 100) | – | S-100 |
| 1 | Styrax officinalis L. seeds oil methyl esters | + 75 ppm aluminum oxide nanoparticle | S-C |
| 2 | Styrax officinalis L. seeds oil methyl esters | + 58 ppm titanium oxide nanoparticle | S-D |
| 3 | Styrax officinalis L. seeds oil methyl esters | + 83 ppm cerium oxide nanoparticle | S-E |

Note: Several trials of each nanoparticle concentration in the range of 50–150 ppm mixed with the biofuel were tested to determine the fuel-blend of each particle type that will give the best engine performance and combustion properties with very low emissions relative to those of biodiesel and conventional diesel-fuels respectively. The biodiesels with the best performance for each particle type were the Styrax officinalis L. methyl esters containing the 75, 58 and 83 ppm $Al_2O_3$, $TiO_2$ and $CeO_2$ nanoparticles respectively.

collected at the top of the separating funnel, while the glycerol was gently decanted via the base of the funnel. To remove traces of biodiesel from the funnel, 10 mL of distilled water was used to thoroughly rinse the funnel. The Styrax officinalis L. biodiesel was then dehydrated with calcium carbonate and centrifuged to remove the associated water. The experiment was conducted in triplicates to ensure repeatability of the measurements with percentage uncertainty within ±0.02. Before commencement of this experiment, all instruments/equipment used were calibrated according to the manufacturers standards.

## 2.2. Preparation of nanoparticles

The nanoparticles used in this work are aluminum, cerium and titanium oxide nanoparticles which were prepared via sol gel method based on the procedures as described in ref. Oni et al. (2021e). The nanofluid preparation lasted for 32 h and the fluids were later treated with distilled water. A Sonics VCX 750 model sonicator was used in mixing the sonicated nanoparticles with the biofuel for a period of 2 h. Ultrasonication helped to homogeneously disperse the nanoparticles in the deionized water as well as the oil in order to form the desired emulsions. Hong et al. (2006) reported that the stability of nanofluids can be enhanced at longer sonication times. Thus, prolonged sonication time prevents and reduces the agglomeration of particles. Ruan and Jacobi (2012) reported that ultrasonication can prevent the agglomeration of particles, thus promoting stable nanoparticles distribution in the base fluids. Furthermore, sodium dodecyl sulfate (SDS) was added to the prepared nanofuel in ratio of (Nanofuel: SDS –1:1, 1:2; 1:3, 1:4) to improve the stability and surface modifications of the nanofuels in order to reduce the tendency for possible coalescence, coagulation and surface tension reduction.

The calibration fluid (deionized water) was used to calibrate the sonicator, three experimental runs were conducted per experiment and the average values of the data generated were tabulated. The sonication time / speed were 80 min150 rpm with a frequency of 50 Hz. The Jenway Models 6305 UV/Vis Spectrophotometer of 115–230 V AC input at 50–60 Hz was used for the absorbance measurements with wavelength range between 220 and 500 nm and corvette dimensions (H x W x D): 42 × 12.5 × 12.5 mm, with an accuracy of ± 2 nm; ± 1%T, ± 0.01Abs at 1.000 Absorbance. The calibration was carried out at the same wavelength at which the sample will be measured.

## 2.3. Characterization of the prepared nanoparticles

The scanning electron microscope (SEM) (Thermofisher scientific Prisma E SEM GX 7330) was used to obtain the surface morphologies of the nanoparticles.

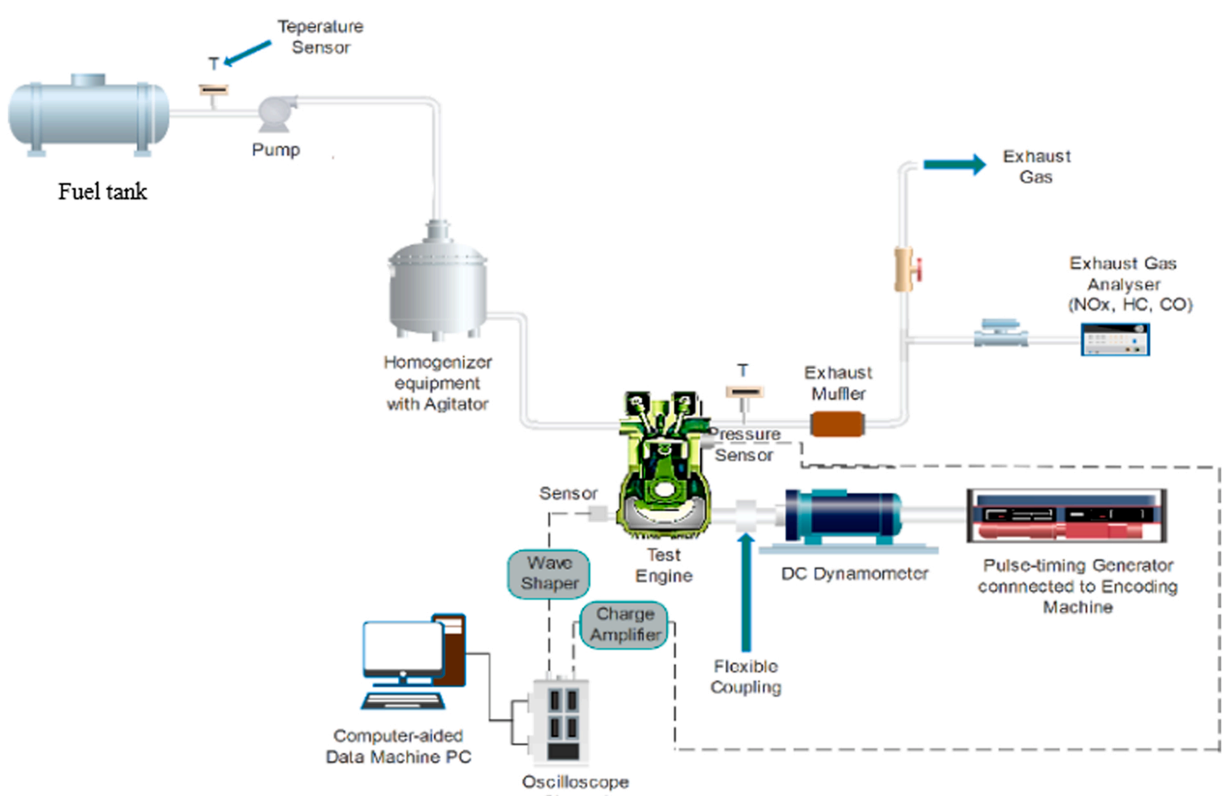


**Fig. 1.** Schematic Illustration of the Lister Petter Engine.

**Table 2**
Lister petter Engine specification.

| Engine type | Lister Petter |
|---|---|
| Engine specification | Single cylinder, naturally aspirated, constant speed, 4 -stroke engine. |
| Capacity ($cm^3$) | 630 |
| Cooling system | Air cooling |
| Stroke and bore length (mm) | 110 × 87.3 |
| Injection pressure (bars) | 210 |
| Number of cylinders | 1 |
| Rated power (kW)/speed (rpm) | 5.2/1500 |
| Compression ratio | 17:1 |
| Diameter of cylinder (mm)Nozzle hole diameter (mm) | 88.90.32 |

**Table 3**
Levels of accuracies of the instruments.

| Engine specification | Accuracy | Range |
|---|---|---|
| Gas analyzer AVL DiComm 4000 | | |
| HC | ±10 ppm | (0 – 5000) ppm |
| CO | ±0.02% | (0 – 9.99) vol% |
| $NO_x$ | ±5 ppm | (0 – 5000) ppm |
| Fuel flow meter | ±0.1 cc | 1–30 cc |
| Pressure transducer | ±0.1 MPa | 0–10 MPa |
| Crank angle encoder | 0.2°CA bTDC | 0 – 720°CA |
| Eddy current dynamometer. | 15 W | 200 – 8000 W |

**Table 4**
The percentage uncertainty of all measured parameters.

| Properties | % Uncertainty |
|---|---|
| Brake specific energy comsumption | 0.2 |
| BTE | 0.3 |
| Nitrogen Oxides | 0.2 |
| Oxides of carbon | 0.1 |
| Pressure | 0.2 |
| Speed | 0.1 |
| Brake power | 0.2 |
| Smoke | 0.1 |
| Hydrocarbon | 0.2 |

### 2.4. The nano-doped fluids

The sol gel technique was used to prepare 300 mg of each nanoparticle (Oni et al., 2021e). 1000 mL of biodiesel fuel was added to the nanoparticles. The mixture was sonicated to ensure that the nanoparticles and biofuel were mixed evenly. The effects of the nanoparticle addition on the characteristics of biodiesel were investigated. The type of fuels used and their blended proportions with the biodiesel are as presented in Table 1.

### 2.5. Testing the fuels in the engine

Fig. 1 shows the Lister Petter test engine whose specifications are as indicated in Table 2. The engine was first fueled with conventional diesel in order to allow the engine to warm up for 20 min. Subsequently, the fuel was evacuated and the different fuel blends (50–150 ppm $Al_2O_3$, $TiO_2$ and $CeO_2$ nanoparticulate fuels) were used as fuels in the engine while being on for 30 min. The process was repeated for all the test-fuels at several load conditions in order to examine the performance, combustion, and emission data retrieved from the engine. The Lister Petter diesel engine properties were checked by a controller connected to a laptop which was synchronized with the test-bed of the engine. The emission properties were measured using the AVL Dicomm 4000-exhaust gas analyzer (Table 3).

**Table 5**
Properties of the prepared nanoparticles.

| S/N | Parameter | $CeO_2$ | $Al_2O_3$ | $TiO_2$ |
|---|---|---|---|---|
| 1. | Mol. weight (g/mol) | 81.39 | 101.96 | 79.87 |
| 2. | Average particle size (nm) | 12 | 11 | 11 |
| 3. | Purity (%) | 99.9 | 99.6 | 99.5 |
| 4. | Colour | Off-white | White | white |
| 5. | Form | Powder | Powder | powder |
| 7. | Surface area, $m^2/g$ | 88.89 | 224.55 | 175 |
| 8. | Density ($kg/m^3$) | 561 | 395 | 432 |

### 2.6. Uncertainty analysis

Accidental errors may occur during experimental tests when taking readings/measurements. Also, a logical error often occurs as a result of poor calibration of measuring equipment. Owing to the several variations in manufactured and designed equipment, which often result in errors from measurements, an uncertainty measurement is therefore necessary during experimentation. The uncertainty evaluation was carried out with repeated experiments (i.e., four runs per experiment) while taking the standard deviation of the measured uncertainty values. The Kline and Mc.Clintock formula was used to evaluate the uncertainties in the experiment used; the results and percentage uncertainties of all measured parameters are as displayed in Table 4.

The formula can be expressed as follows:

$$\Delta T = [(\frac{\partial T}{\partial y_1}\Delta y_1)^2 + (\frac{\partial T}{\partial y_2}\Delta y_2)^2 + \ldots + (\frac{\partial T}{\partial y_n}\Delta y_n)^2]^{\frac{1}{2}} \quad (1)$$

Where $\Delta T$ = the total uncertainty.

T – depends on the independent variables of $y$, $y_2$ ………… $y_n$

$\Delta y_1, \quad \Delta y_1 \ldots\ldots\ldots \quad \Delta y_1 \quad are \quad the \quad independent \quad variable \quad uncertainties.$

From the experimental result, the total uncertainty was calculated within the limit of ±0.32%.

## 3. Results and Discussion

### 3.1. Characteristics of the NPs

To determine the average particle size of all nanoparticles used, the HMK-22 Fisher Sub Sieve Sizer- microns /Average Particle Size Analyzer (Fisher Model 95 (Model 14–311 A) was used. The particle size of the $CeO_2$ nanoparticles was the highest (12 nm), while nanoparticles of $Al_2O_3$ and $TiO_2$ were of size 11 nm each. Using HPLC-mass spectrometry, the purity of each metallic oxide (nanoparticle) was determined. From the results, $CeO_2$ nanoparticles displayed the highest purity of 99.9% whereas $Al_2O_3$ and $TiO_2$ gave 99.6% and 99.5% purities. The Brunauer–Emmett–Teller (BET) Horiba SA-9600, BET multipoint surface area analyzer, HORIBA Scientific method was used to examine the particle's surface area. By carrying out $N_2$ multilayer adsorption as a function of relative pressure, a thorough specific surface area evaluation of the materials was ensured. The method provides information on how gas molecules adsorb onto a solid surface. The surface area measured for all nanoparticles of $CeO_2$, $Al_2O_3$ and $TiO_2$ are 88.9, 224.55 and 175 $m^2/g$ respectively. The $Al_2O_3$ nanoparticle gave the highest surface area amongst others. The densities of the nanoparticles were calculated in terms of mass per unit volume (Table 5) in the order of $CeO_2$ >$TiO_2$ >$Al_2O_3$. All nanoparticles used in this work were in powder form. In terms of color, the $Al_2O_3$ and $TiO_2$ nanoparticles were white, whereas $CeO_{2\ looked}$ off- white. Since molecular weight is a measure of the sum of the atomic weight values of the atoms in a molecule, the molecular weight of $Al_2O_3$ (101.96 g/mol) is higher than that of $CeO_2$ (81.39 g/mol) and $TiO_2$ (g/mol). Finally, the $CeO_2$ was denser than the other metal oxides considered in the study with its measured density being 561 $kg/m^3$. The density recorded for the $Al_2O_3$ and $TiO_2$ nanoparticles

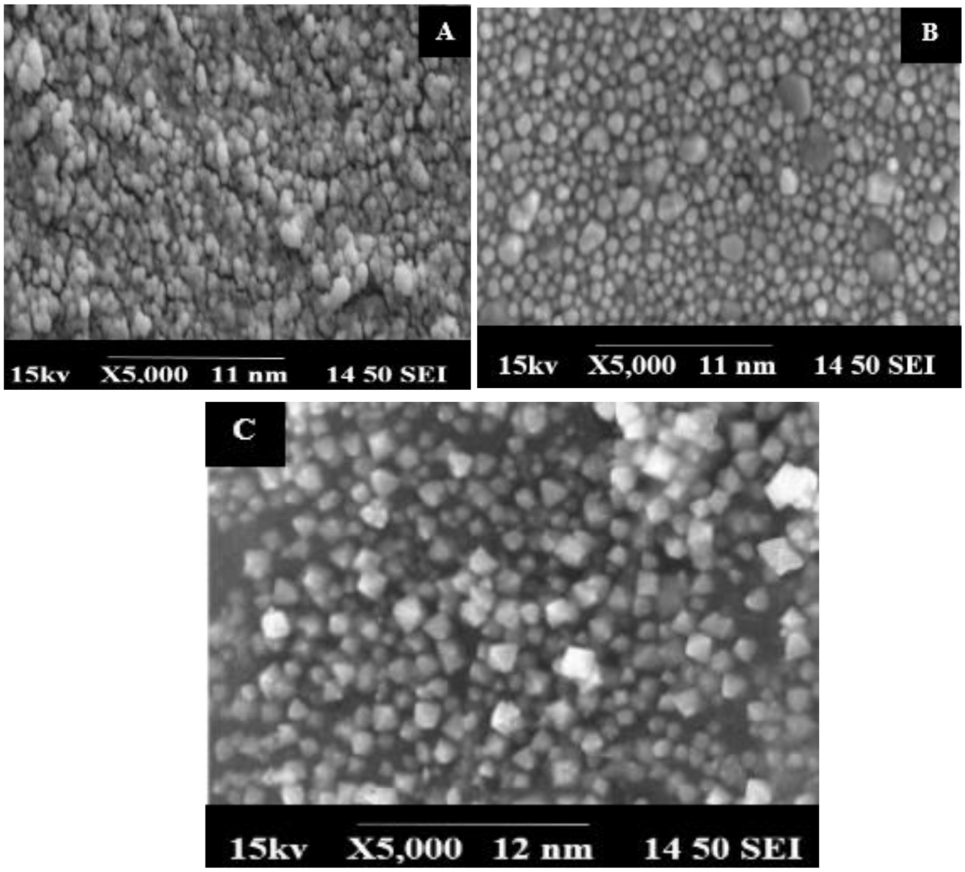


**Fig. 2.** SEM images of nanoparticles: (a) $Al_2O_3$ (b) $TiO_2$ (c) $CeO_2$.

are 395 and 432 kg/$m^3$.

### 3.2. Characterization of the nanoparticles

Fig. 2(a-c) shows the SEM images of the prepared NPs. The porous structures of the NPs were determined by observing the surface morphologies of the nanoparticles, which showed their textural and pore size arrangements. The morphologies of the NPs were determined using the micrographs of the scanning electron microscope (SEM). The nano-dispersed forms of the NPs are as shown in Fig. 2a, b, and c. The particles appear clumped together. Despite the fact that nanomaterials always stick together and form agglomerates (unless properly treated), protrusions can be seen in Fig. 2a and c, which are common in nanomaterials. In addition, increased levels of blunt sponge-like protrusions were observed in Fig. 2b, which could be a possible reason for the NPs' compatibility with the Styrax officinalis L. methyl ester.

### 3.3. Nanoparticle stability

The inducement of the stability of a nanoparticle is very important because it helps to prevent the blockage of the nozzles in engines. Fig. 3a-c show the weekly stability-measurements of the NP-surfactant blends (C:SDS, D:SDS and E:SDS) with the possibility of reducing surface tension, coalescence and coagulation. Based on data obtained from the Ultraviolet/Visible (UV/Vis) spectrophotometry, as the time duration increased, the absorbance reduced for all the nanoparticles mixed with SDS. At the end of every week, the nanofluids were kept under static conditions while their absorbances were measured, and at the end of the eighth week, the absorbance curve flattened. The nanoparticles were used immediately, to prevent further agglomeration which may likely occur.

Table 6 represents the physicochemical properties of all the test-fuels. The measured properties are densities, cetane number, pour, flash and cloud points, kinematic viscosities, and calorific value. Low viscosities, higher cetane number, and moderate calorific values are associated with these nanofuels when compared with the conventional diesel fuel. These properties in the nanofuel improved the fuel characteristics in terms of combustion, emissions and performance in the Lister Petter Engine.

The densities of the fuels increase in the following order; S-D (817.1) < S-E (818.2) < *S-C* (819.0) < *D-100* (827.3) < *S-100* (842.5) kg/$m^3$; D-100 which is the neat conventional diesel is less dense than the neat biodiesel fuel due to the FFA and oxygenates in the biodiesel. The nanofuels gave lower densities as a result of the presence of metal oxide nanoparticles in the biodiesel; these results corroborate the findings of ref. Oni et al. (2021e). The diesel fuel gave high calorific value compared to other fuels , while the neat biodiesel gave the least calorific value. There was a remarkable improvement in the nanofuels' calorific values compared to those of the neat biodiesel, which is an indication that the nanoparticles have the capacity to increase the neat biodiesel's calorific value; this justifies the findings of ref. Oni et al. (2022). Cetane number measures the quantity/performance of diesel fuel. Higher cetane number increases the fuel's burning property within the vehicle. The cetane number of the fuels increased in the following order; S-D (51.1) < S-E (50.9) < *S-C* (50.3) < *S-100* (49.1) < *D-100* (48.4).

Other properties measured in Table 6 include; flash point, cloud point, pour, point and kinematic viscosity. The temperature at which the fuels goes into vapor phase when in contact with an igniting source is its flash point. All the tested fuels gave flash points between 54 and 152 °C with the neat biodiesel having the highest flashpoint temperature of 152 °C. Upon the addition of nanoparticle to the biodiesel fuel, the flashpoint was seen to decrease marginally as shown in Table 6. Based

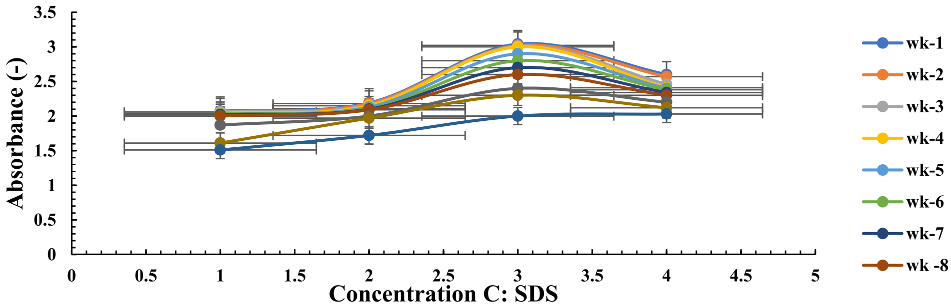


(a)

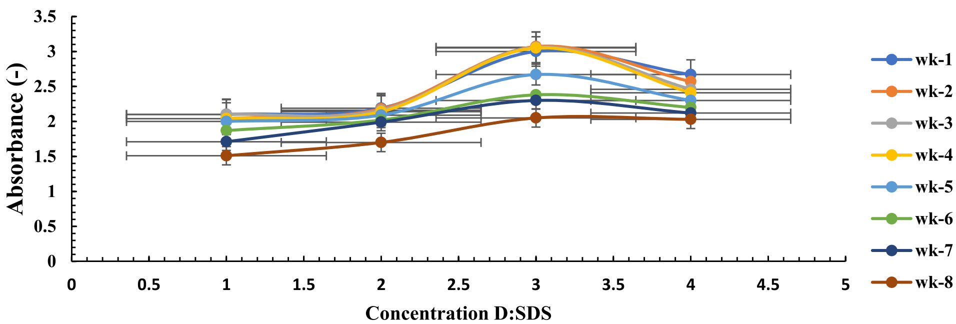


(b)

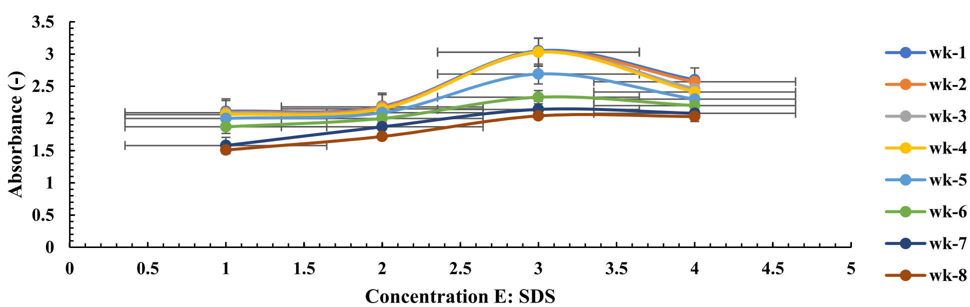


(c)

**Fig. 3.** a) Absorbance vs concentration of C: SDS (1:1, 1:2; 1:3, 1:4). b) Absorbance vs concentration of D: SDS (1:1, 1:2; 1:3, 1:4). c) Absorbance vs concentration of E: SDS (1:1, 1:2; 1:3, 1:4).

**Table 6**
Physicochemical characteristics of Diesel, Styrax officinalis L. biodiesel and Styrax officinalis L. biodiesel - nanoparticle blends.

| Parameter | D-100 | S-100 | S-C | S-D | S-E | ASTM method |
|---|---|---|---|---|---|---|
| Flash point (°C) | 54 | 152 | 77 | 68 | 56 | D-93 |
| Kinematic viscosity @ 40 ($mm^2/s$) | 3.99 | 5.3 | 3.22 | 3.19 | 3.02 | D-445 |
| Calorific Value (MJ/kg) | 45.15 | 42.02 | 43.00 | 42.99 | 43.19 | D-240 |
| Density kg/$m^3$ | 827.3 | 842.5 | 819.0 | 817.1 | 818.2 | D-1298 |
| Cetane number | 48.4 | 49.1 | 50.3 | 51.1 | 50.9 | D-613 |
| Pour point (°C) | -4 | 9 | 3 | 1 | -2 | D-2500 |
| Cloud point (°C) | -2 | 5 | 1 | -1 | -1 | D-2500 |

on the results obtained on kinematic viscosities (viscosities/densities) in Table 6, the kinematic viscosities of the nanofuels were lower relative to those of the neat diesel and biodiesel fuel. The kinematic viscosities of the fuels are 3.99, 5.3, 3.22, 3.19, 3.02 $mm^2/s$ i.e., for the D-100, S-100, S-C, S-D and S-E respectively. High fuel viscosity can lead to low BTE, poor atomization, longer ignition delay, poor mixing with air, higher emissions and low peak pressure (Ettefaghi et al., 2018; Basha and Anand, 2011). Viscosity is an important parameter in terms of fuel evaporation and combustion. The lowest temperature at which a fuel will flow is called its pour point. Diesel fuel gave the lowest pour point of − 4 °C. All the nanofuels gave moderate pour points, while the neat biodiesel's pour point was 9 °C. The fuel's cloud points increased in the following order of magnitude: S- 100 (5 °C) < S-C (1 °C) < *S-D* (−1 °C) < *S- E* (−1 °C) < *D-100* (−2 °C) respectively.

### 3.4. *Performance characteristics*

#### 3.4.1. *Brake thermal efficiency (BTE)*

Fig. 4 shows the brake thermal efficiencies of all the test-fuels at various load conditions. The efficiency with which a fuel's chemical energy is turned into practical work in an engine is known as the brake thermal efficiency (BTE). BTE is inversely proportional to brake specific energy consumption (BSEC) and the low heating value of a fuel (Ors et al., 2018). Also, low BTE of biodiesels can occur as a result of high

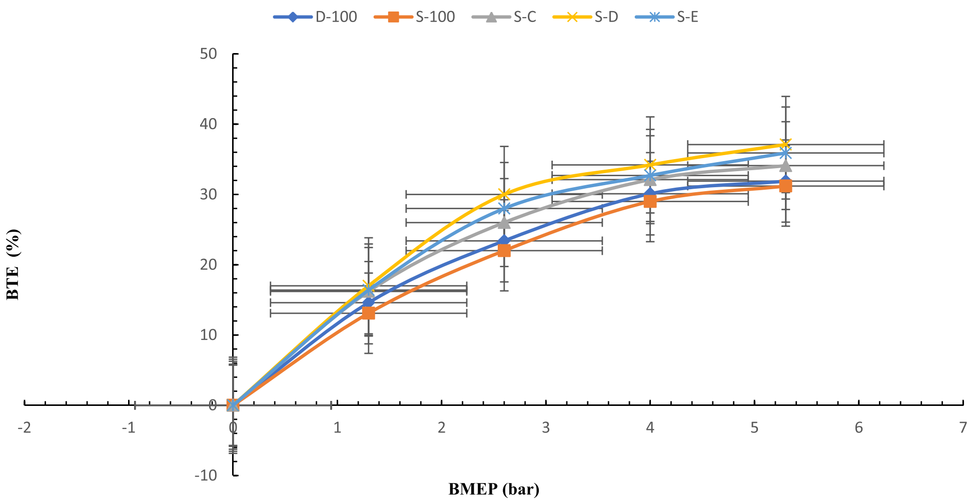


**Fig. 4.** BTE vs engine load for the Lister petter Engine.

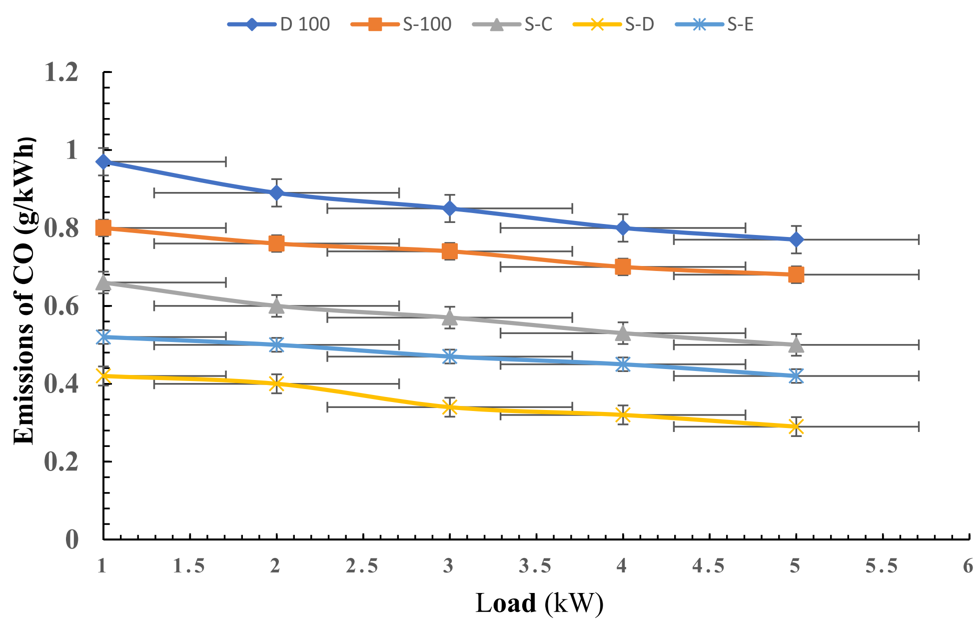


**Fig. 5.** CO vs engine load for the Lister petter Engine.

viscosities and densities, as well as lower calorific values relative to those of diesel, which is majorly responsible for the lower BTEs of the tested pristine biodiesel. The results showed that the BTE increased with the addition of nanoparticles for all the fuels due to the higher temperature in the combustion chamber as a result of the presence of NPs in the biodiesel, thus leading to improved BTEs. Furthermore, the BTEs of the blended fuels are higher than that of the neat biodiesel, as a result of the enhanced fuel combustion, vaporization, and atomization imposed by the different nanoparticles. Furthermore, the traces of $O_2$ present in the nano metallic oxides aided the complete combustion of the fuel blends, thus increasing their BTEs. The highest attained BTEs for the biodiesel admixed in the various proportions and compositions of the S-C, S-D, and S-E are 34.1%, 37.1% and 35.9% respectively compared to those of the neat biodiesel and diesel fuel whose BTEs are 31.2% and 31.9% respectively. Adding nanoparticles to the neat biodiesel decreased the viscosities of the blends and thus improved the geometry of the fuel spray and atomization. These results are in line with the results of refs. Soudagar et al. (2018), Ettefaghi et al. (2018) and Ghanbari et al. (2017).

### 3.5. *Emission characteristics*

#### 3.5.1. *Carbon (II) oxide emission*

Fig. 5 illustrates the variations of carbon monoxide emissions at various engine loads of the Lister Petter engine with and without NPs in the biodiesel. The carbon monoxide emissions of the blends are lower than those of the Styrax officinalis L. methyl ester and diesel fuel. These are as a result of the higher gas temperatures within the combustion chamber wall at the pre-mixed stage, which in turn lowers the amount of CO released. It was also discovered that at 100% load condition, the blends gave lower CO emissions compared to the diesel and biodiesel without nanoparticles. This could be due to an increase in the amount of excess $O_2$ in the blends which may have resulted in complete combustion and oxidation of carbon (II) oxide into carbon (IV) oxide. The CO emissions of the S-C, S-D, and S-E at full load conditions are 0.5, 0.29 and 0.42 g/kWh respectively, which are lower than those of the neat biodiesel and diesel fuels whose values are 0.68 and 0.77 g/kWh respectively. These results corroborate the findings in refs. Morone and Yilan (2020) and Praveen et al. (2017). Higher $O_2$ levels in the fuel-rich combustion zone are thought to promote further complete

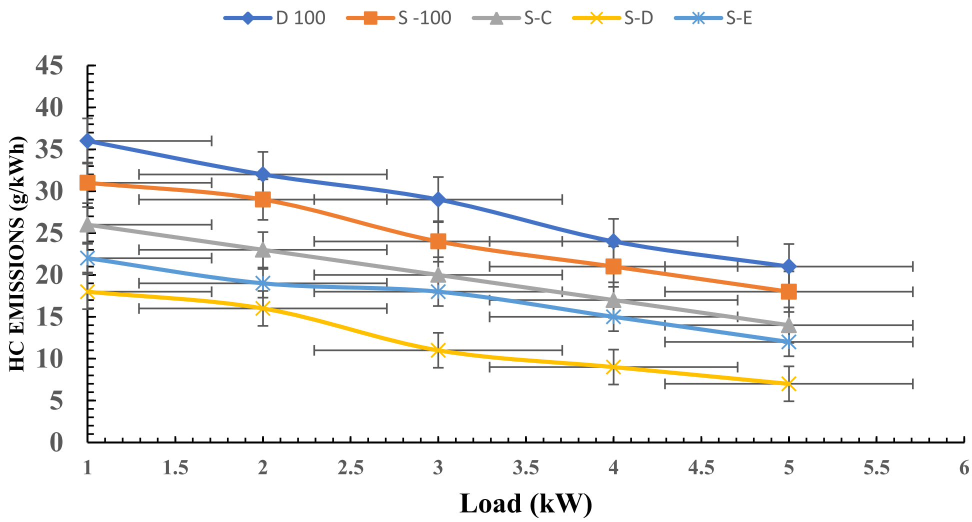


**Fig. 6.** HC vs engine load for the Lister petter Engine.

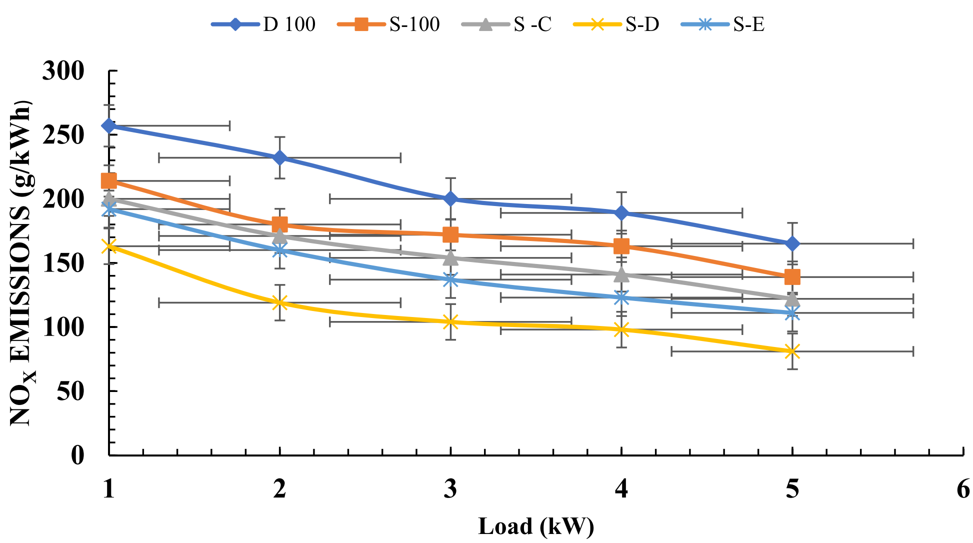


**Fig. 7.** HC vs engine load for the Lister petter Engine.

combustion, thus lowering CO concentrations in the exhaust emissions. Because of complete combustion, CO decreases as load increases. In each operating mode, S-D emitted the least CO compared to all the other test-fuels.

### 3.5.2. *Hydrocarbon emissions*

Unburned HCs are produced when fuel combustion is incomplete. Fig. 6 shows the variations in HC emissions with engine loads for the Lister petter engine with and without nanoparticle addition in the fuels. The hydrocarbon emissions of the blended fuels are lower than those of the neat biodiesel and diesel fuel. These can also be ascribed to the increased post combustion temperature which leads to heat loss reduction in the cooling system. Additionally, the blends of Styrax officinalis L. methyl ester with NPs significantly decreased the HC emissions due to the availability of excess oxygen in the blends, thus improving the fuel quality and enhancing complete combustion. Styrax officinalis L. seed oil biodiesel admixed with nanoparticles enhanced the biofuels' evaporation rate thus allowing for better mixing which leads to the reduction of HC emissions with improved combustion properties. The hydrocarbon emissions of the blends are 14, 7 and 12 g/kWh S-C, S-D and S-E respectively compared to those of the neat biodiesel and diesel fuel whose HCs are 18 and 21 g/kWh respectively; these results corroborate the findings of refs. Oni et al. (2021e), Dubey et al. (2019) and Basha and Anand (2011).

### 3.5.3. *$NO_x$ emissions*

The $NO_x$ emissions for all the fuels used in the Lister Petter engine at varying load conditions are as illustrated in Fig. 7. There is a continuous decrease in the $NO_x$ emission with an increase in the engine load as a result of the higher combustion temperature inherent in the combustion chamber; this may also be due to the shorter residence time available for $NO_x$ formation. Additionally, the $NO_x$ emission for the blended fuels at higher loads are lower than those of the neat biodiesel and diesel fuels. The nanoparticles admixed with the biodiesel imposed shorter ignition delays despite the presence of oxygen in the methyl esters. Also, the nanoparticle-additives reduced $NO_x$ formation at higher gas temperatures. The overall $NO_x$ emissions for all the blended fuels S- C, S-D and S-E are 122, 81 and 111 g/kWh respectively as compared with those of the neat biodiesel and diesel fuel whose values are 129 and 165 g/kWh respectively at full load condition; these results corroborate the findings in refs. Ettefaghi et al. (2018) and Hong et al. (2006).

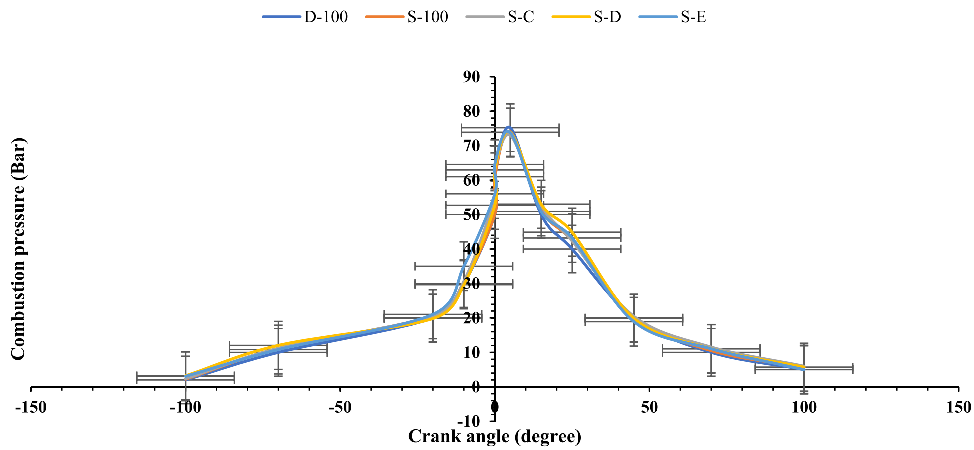


**Fig. 8.** In-cylinder pressure vs Crank angle for Lister petter Engine.

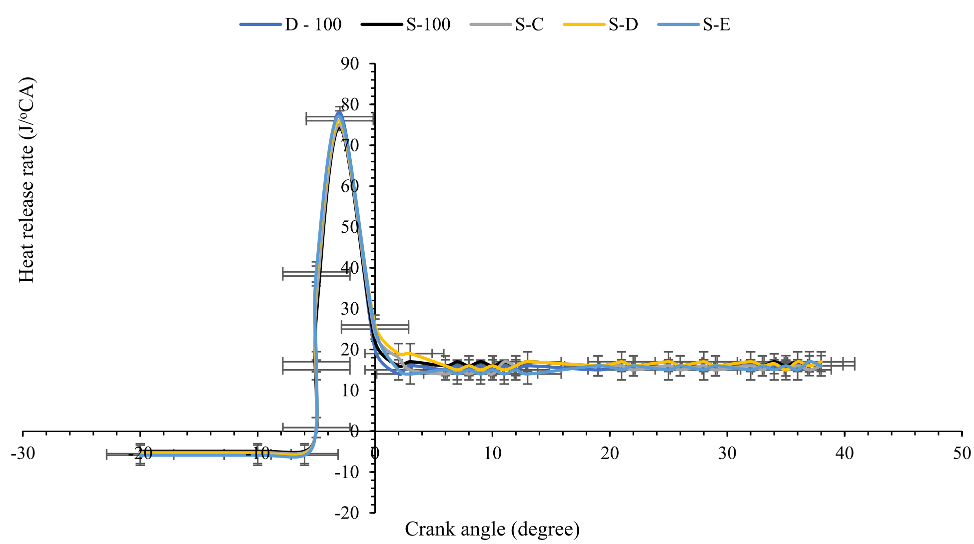


**Fig. 9.** HRR vs crank angle for all the fuels.

### 3.6. Combustion characteristics

#### 3.6.1. Combustion pressure

The in-cylinder gas pressure data is critical for evaluating how heat energy is converted into useful work according to the first law of thermodynamics. The ability of the fuel to combine with air and the rate of combustion during the premixed combustion phase are measures of the in-cylinder pressure. The plot of the combustion pressure curve for all the test-fuels at full-load under varying crank angles is shown in Fig. 8. At full load condition, the reduction in peak pressure is proportional to the amount of biodiesel in the blends. The in-cylinder pressure history has a direct impact on the engine's characteristics, and it is important to understand how the combustion process works. In comparing the blended fuels to diesel, the averaged pressures are lower for the blends. The average peak in-cylinder pressures of 73, 73.9 and 73.8 bar were observed for the blends, while those of the diesel and neat biodiesel fuels are 75.2 and 74.0 bar respectively; this agrees with the findings in ref. Chuah et al. (2016). The higher peak in-cylinder pressure of the diesel may be as a result of its lower volatility due to its larger density, which results in poor air-fuel mixing and incomplete combustion. The nano-fuels reduced the ignition delay period of the engine, which has a significant impact on the engines combustion as well the rate of pressure rise. Longer ignition delays are usually responsible for faster and greater rates of pressure rise. With the addition of nanoparticles to the biodiesel, there were reduced/shortened chemical and physical ignition delays, thus, resulting in a decrease in peak pressures of the nano-fuels. As a result of the increased ignition capabilities of energetic nanoparticles, early fuel-combustion was initiated, which in turn lowered the resulting peak pressures. The decrease in in-cylinder pressure of the nano-fuels may also be attributed to the progress of the premixed combustion zone.

Fig. 9 illustrates the HRR variation with crank angle for all the tested fuels at 100% load. Due to the initiation of fuel vaporization during the delay period, the HRR curve initially exhibited a negative trend. HRR demonstrates a predominance of premixing and diffusion during combustion. Due to the shorter ignition delays, the premixed stage for Styrax officinalis L. biodiesel admixed with nanoparticles was shorter compared to that of the diesel fuel. The maximum HRR for the diesel was recorded as 78 J/°CA, whereas, those of the nano-fuels are 75, 77, and 76 J/°CA for the S-C, S-D, and S-E, respectively, thus indicating that the HRR decreased for the blended fuels, whereas there was a slight increase when compared to that recorded for the neat biodiesel. The peak crank angle is about − 3 °CA for the S-E and − 5 °CA for the D-100 fuel.

The HRR decreased for the premixed combustion phase, whereas, it increased in the diffusion phase. The nano-fuels also exhibited increased cetane numbers which corresponded to shorter ignition delays. The presence of nanoparticles tends to absorb the engine cylinder temperature due to the high thermal conductivities of NPs.

The results from other works compared to those obtained in this study are as shown in Table 7. Tables 8 and 9 present the cost of biodiesel production from other works using various technologies and

**Table 7**
Compared data from other works with those of this study.

| Engine specification | Engine speed and CR | Nanoparticle/size | Nanoparticle dosage | Biodiesel blend | Performance compared to diesel | Emission properties | Economic advantage of this approach | Economic disadvantage of this approach | Refs. |
|---|---|---|---|---|---|---|---|---|---|
| Kirloskar (TV1), 220 bars DI engine, Single cylinder, four -stroke, | 1500 rpm; 17:1 | $TiO_2$; 30–50 nm | 50 ppm $TiO_2$; | CalophyllumInophyllum biodiesel | BTE ↑ | NOx ↓,HC ↓ CO ↓ | Economically feasible. Providing a higher net annual profit (NNP) after taxes and more after-tax rate of return (ARR), with capacity of 100 000 tons year-1 | High capital cost to set up plant is required. | (Ruan and Jacobi, 2012) |
| Kirloskar (AV1), water cooler, 220 bars, four-Stroke, single cylinder. | 1500 rpm; 17:1 | hybrid $MnO_2$:$Al_2O_3$; $CeO_2$: CuO; ZnO: $TiO_2$;$TiO_2$:$Al_2O_3$, | 1:1, 1:3, 1:2 and 2:1 | Juliflora biodiesel | BTE ↑ | NOx ↓,HC ↓ CO ↓ | Economically feasible, since optimizingextraction process could provide better breakeven price of biodiesel | There are high cost implications if Acid catalyzed transesterification is used to esterify the free fatty acid into biodiesel | (Oni et al., 2021e) |
| Kirloskar, Single cylinder, four-stroke, AC, | 1500 rpm;17.5:1 | $CeO_2$ and $Al_2O_3$ | $Al_2O_3$/ $CeO_2$, 50, 32 nm | Jojoba biodiesel | BTE ↑ BSEC↓ | CO ↓ NOx ↓,HC ↓ | It is relatively expensive. Not economically feasible. | Factors such as capital cost, plant capacity, process technology, raw material cost andchemical costs, may be difficult to achieve especially in developing countries for easy start-up | (Oni et al., 2022) |
| AV1-Kirloskar, four-Stroke, single cylinder,230 BTDC, 210 bars | 1500, 16.5:1 | $Al_2O_3$;30 nm | 50–100 ppm; | Pongamia biodiesel | BTE ↑ | NOx ↓,HC ↓ smoke ↓, CO ↓ | – | – | (Ors et al., 2018) |
| AV1-Kirloskar, Single-cylinder, water cooler, four -stroke, 23°BTDC, 220 bars | 1500 rpm; 17:1 | Graphene Oxide;23 – 27 nm | 40 – 60 ppm graphene oxide; | Simarouba biodiesel | BTE ↑ | NOx ↓, smoke ↓, HC ↓ CO ↓ | – | – | (Ghanbari et al., 2017) |
| Kirloskar (AV1), 4- Stroke, 220 bars, water cooler, single cylinder, | 1500 rpm; 16:1 | CeO2; 25 nm | Acetyl-ferrocene,Ac/ 2Fe and PdL | Canola Oil biodiesel | BTE ↑ | CO ↓ NOx ↓,HC ↓ | Economically feasible, since raw materials are readily available. The additives also improved the biodiesel quality and contains less free fatty acids. Requires minimum cost of input materials usuallycatalysts | – | (Praveen et al., 2017) |
| Lister Petter Engine | 1500 rpm; 17:1 | $Al_2O_3$, $TiO_2$ and ZnO; 12,11,11 | 75, 58 and 83 ppm, | Styrax officinalis L. seed oil methyl esters | BTE ↑ | CO ↓ NOx ↓,HC ↓ | Economically feasible using alkali catalystthan biocatalysts with lower fixed capital cost. The plant cost requires using this catalyst is relatively cheaper than other catalyst which is about 68.3% higher. | The inclusion of nanoparticle added to the initial cost of production of the biofuel. However, compare to the advantages the NPs offer in the biofuel, the cost is affordable. | This work |

 

**Table 8**
The cost of biodiesel production from other works using various technologies and different feedstocks.

| Type of production technology | Plant capacity | Type of feedstock used | Estimated Cost of production $/ton | Ref. |
|---|---|---|---|---|
| Lipase catalyzed transesterification | 8000 ton/year | WCO | 1048.00 | (Karmee et al., 2015) |
| Potassium hydroxide catalyzed transesterification with $CH_3OH$ | | WCO | 869. 00 | |
| Sulphuric acid catalyzed transesterification with $CH_3OH$ | | WCO | 750.00 | |
| Homogeneous Sulphuric acid catalyzed | – | Oil from microalgae | 580.00 | (Brunet et al., 2012) |
| | | Oil from microalgae | 620.00 | |
| KOH catalyst process | 1000 ton/ year; batch mode | PO | 1167.00 | (Jegannathan et al., 2011) |
| Catalyst process from immobilized lipase | | PO | 2415.00 | |
| Catalyst process from lipase | | PO | 7821.00 | |
| Purification process from hot water + potassium hydroxide catalyst | 1452 ton/ year; batch mode | WCO | 920.00 | (Sakai et al., 2009) |
| Heterogeneous calcium oxide catalyst using the vacuum fatty acid methyl esters distillation. | | WCO | 970.00 | |
| Potassium hydroxide catalyst + using the vacuum fatty acid methyl esters distillation. | | WCO | 985.00 | |
| Heterogeneous calcium oxide catalyst + purification process from hot water | | WCO | 913.00 | |
| Sodium hydroxide catalyzed transesterification with $CH_3OH$ | | Styrax officinalis L. methyl ester | 874. 00 | This study |

*WCO – waste cooking oil; *PO - palm oil

different feedstocks as well as the cost of biodiesel production from Styrax officinalis L. methyl ester $/ton.

The strengths and limitations of this work are reported in Table 10.

## 4. Conclusion

The results from the investigation validate the consideration of Styrax officinalis L. biofuel as a potential fuel for diesel engines. Fuel properties such as pour point, density, viscosity, flash point, and cetane number of Styrax officinalis L. biodiesel blended with nanoparticles and conventional diesel were somewhat modified which imparted positively on the engine performance, exhaust emissions and combustion characteristics. The experimental tests conducted on the performance, combustion and emission characteristics of the biodiesel blended with nanoparticles in different proportions validate the suitability of $Al_2O_3$, $CeO_2$, and $TiO_2$ NPs as performance enhancers in the Lister Petter engine, thus confirming that the nano-fuels (Styrax officinalis L. biodiesel admixed $Al_2O_3$, $CeO_2$, and $TiO_2$ NPs), are more environmentally friendly and ensure efficient utilization of energy in the engine. Other conclusions are as follows:

**Table 9**
Cost of biodiesel production from Styrax officinalis L. methyl ester $/ton.

| Expenses | Price ($) | Quantity | Cost ($) |
|---|---|---|---|
| **Raw material** | | | |
| Styrax officinalis L. oil | 0.51/kg | 1000 | 551.00 |
| NaOH | 1.85/kg | 9 | 16.65 |
| $CH_3OH$ | 0.45/kg | 265 | 119.25 |
| Tap water | 2.20/ton | 140 | 2.2 |
| $CaCO_3$ | 0.2/kg | 2 | 0.4 |
| **Utilities** | | | |
| Manpower | Manpower | 3 | 120 |
| Steam | 0.03/kg | 1800 | 54 |
| Electricity | 0.110/kWh | 8.1 | 0.891 |
| **Total** | | | **864.241** |
| **Byproducts** | | | |
| Glycerol | 1.6/kg | 48 | **76.8** |
| **Total** | | | **787.441** |
| Depreciation | 6% | – | 47.25 |
| Repair | 2.5% | – | 19.69 |
| Interest and tax | 2.5% | | 19.69 |
| **Grand total** | | – | **874.071** |

**Table 10**
Strength and limitations of the work.

| | Strengths | Weakness |
|---|---|---|
| 1 | The nanosuspension (nanoparticle-biofuel biofuel mix) was stabilized within 8 weeks, due to the properties of the biodiesel. Some reports from literature (Oni et al., 2021e, 2021a; Soudagar et al., 2018) were for 11, 12 and 13 weeks, however the properties of the fuels were highly comparative with those obtained in this study. Also, after 8 weeks the particles retained their stability. | Efforts were made to increase the BTE of other nanofuel, Styrax officinalis L. seeds oil methyl esters + 75 ppm $Al_2O_3$ nanoparticle (S-C) (34.1%), and Styrax officinalis L. seeds oil methyl esters + 58 ppm titanium oxide nanoparticle (S-E) (35.9%) as well as reducing the level of emissions by varying their concentrations in the biodiesel, as there was no further increase in BTE/decrease in emission, despite increasing/decreasing their concentrations in the biodiesel. Thus, Styrax officinalis L. seed oil methyl esters + 58 ppm titanium oxide nanoparticle (S-D) displayed the best nanofuel amongst others. |
| 2 | One of the nanofuels i.e., the (S-D) sample attained the highest BTE of 37.1%, whereas, the works of refs. [16–19, 23, 24] reported that the nanofuels from other literature gave lower BTEs. | The neat biodiesel alone is not suitable in CI engines when compared to the nanofuels, due to its poor performance, poor emissions and poor physicochemical properties. |
| 3 | The properties of the nanofuels include moderate viscosity, density, flash point, higher cetane number etc. These properties ensure the suitability of the nanofuel which reduces the ignition delay period, improves the combustion properties as well as the fuel performance upon operation in the CI engine. High viscosity of the fuel can lead to low BTE, poor atomization, longer ignition delay, poor mixing with air and often times higher emissions and low peak pressures. | It was observed that the least performed nanofuel (S-C) gave weaker properties which negatively affected its flash point, cetane number and viscosity with longer ignition delay relative to that of the S-D fuel. |
| 4 | In terms of emissions, there is an appreciabel marginal decrease in the level of emissions of the nanofuel when compared to that of the diesel fuel. | Despite the lower HC and CO, higher NOx emissions were recorded for the S-C (200 g/Kw/h) and S-E (192 g/kWh) fuels relative to that of S-D (163 g/kWh). |

(i) The nano-fuels demonstrated lower HC, CO, and $NO_x$ emissions compared to those of the conventional diesel and neat biodiesel fuels.
(ii) The engine performance increased for all the nano-fuels, in which the nano-doped Styrax officinalis L. biodiesel doped with $TiO_2$ nanoparticles gave the best improved properties amongst all the fuel blends in terms of the recorded BTEs, emissions and combustion characteristics.
(iii) The addition of the different nanoparticles to the biodiesel improved the fuels' physicochemical characteristics such as flash point, kinematic viscosity, pour point, cetane number, density and cloud points.
(iv) Shorter ignition delay periods were recorded in the nano-fuels as a result of their in-cylinder pressures and HRRs.
(v) Overall, the results showed that the nano-fuels can be used satisfactorily as fuel sources to power the Lister Petter diesel engine.
(vi) The performance of the nano-fuels in the engine are in the following order: S-D (Sytrax officinalis L biodiesel + 58 ppm $TiO_2$ nanoparticles) > S-E (Sytrax officinalis L biodiesel + 83 ppm $CeO_2$ nanoparticles) > S-C (Sytrax officinalis L biodiesel + 75 ppm $Al_2O_3$ nanoparticles) > D-100 (neat diesel) > S-100 (neat biodiesel), which is thus indicative of the superiority of the S-D fuel-sample relative to other fuel samples in terms of the measured BTEs.

## CRediT authorship contribution statement

**Babalola Aisosa Oni:** Conceived the idea, carried out the experimentation, Made the first draft copy of the manuscript, Result analysis and Data curation. **Samuel Eshorame Sanni:** Made useful contributions at different stages of the research, Involved in recomposing key sections of the manuscript and general editing. **Anayo Jerome Ibegbu:** Made very vital/useful observations at the experimental design and experimentation stages. **Tomiwa I. Oguntade:** Data curation and result analysis

## Declaration of Competing Interest

The authors declare that they have no known competing financial interests or personal relationships that could have appeared to influence the work reported in this paper.

## Acknowledgement

The authors wish to appreciate OBA 1 group for their assistance at the experimental stage as well as helping is sourcing for the raw materials needed for this project.

## References

Agbulut, Ü., Karagoz, M., Sarıdemir, S., Oztürk, A., 2020. Impact of various metal-oxide based nanoparticles and biodiesel blends on the combustion, performance, emission, vibration and noise characteristics of a CI engine. Fuel 270, 117521 doi.org/10.1016/j.fuel.2020.117521.

Basha, J.S., Anand, R., 2011. An experimental study in a CI engine using nonadditive blended water–diesel emulsion fuel. Int J. Green. Energy 8 (3), 332–348 doi.org/10.1080/15435075.2011.557844.

Brunet R., Carrasco D., Muñoz E., Guillén-Gosálbez G., Katakis I., Jiménez L. Economic and environmental evaluation of microalgae biodiesel production using process simulation tools. In: Symposium on computer aided process engineering; 2012. p. 20. Doi.10.1016/j.cherd.2012.05.001.

Chuah, L.F., Yusup, S., Aziz, A.R.A., Klemeš, J.J., Bokhari, A., Abdullah, M.Z., 2016. Influence of fatty acids content in non-edible oil for biodiesel properties. Clean. Technol. Environ. Policy 18 (2), 473–482 doi.org/10.1007/s10098-015-1022-x.

Dogana, B., Cakmak, A., Yesilyurtc, M.K., Erold, D., 2020. Investigation on 1-heptanol as an oxygenated additive with diesel fuel for compression-ignition engine applications: An approach in terms of energy, exergy, exergoeconomic, enviroeconomic, and sustainability analyses. Fuel 275, 117973. DOI:10.1016/j.fuel.2020.117973.

Dubey, R.S., Krishnamurthy, K.V., Singh, S., 2019. Experimental studies of $TiO_2$ nanoparticles synthesized by sol-gel and solvothermal routes for DSSCs application. Res Phy 14, 102390 doi.org/10.1016/j.rinp.2019.102390.

Ettefaghi, E., Ghobadian, B., Rashidi, A., Najafi, G., Khoshtaghaza, M.H., Rashtchi, M., Sadeghian, S., 2018. A novel bio-nano emulsion fuel based on biodegradable nanoparticles to improve diesel engines performance and reduce exhaust emissions. Renew. Energy 125, 64–72 doi.org/10.1016/j.renene.2018.01.086.

Gebremariam, S.N., Marchett, J.M., 2018. J.M Economics of biodiesel production: review. Energy Convers. Manag. 168, 74–84 doi.org/10.1016/j.enconman.2018.05.002.

Ghanbari, M., Najafi, G., Ghobadian, B., Yusaf, T., Carlucci, A., Kiani, M.K.D., 2017. Performance and emission characteristics of a CI engine using nano particles additives in biodiesel- diesel blends and modeling with GP approach. Fuel 202, 699–716 doi.org/10.1016/j.fuel.2017.04.117.

Gowtham, M., Prakash, R., 2020. Control of regulated and unregulated emissions from a CI engine using reformulated nano fuel emulsions. Fuel 271, 117596 doi.org/10.1016/j.fuel.2020.117025.

Hasan, M.M., Rahman, M.M., 2017. Performance and emission characteristics of biodiesel-diesel blends and environmental economic impacts of biodiesel production: a review. Renew. Sustain Energy Rev. 74, 938–948.

Hong, K.S., Hong, T., 2006. Thermal conductivity of Fe nanofluids depending on the cluster size of nanoparticles. Appl. Phys. Lett. 88, 031901 doi.org/10.1063/1.2166199.

IEA, 2015. Medium Term Renewable Energy Market Report 2015, Executive Summary: Market Analysis and Forcasts to 2020. International Energy Agency,.

Jegannathan, K.R., Eng-Seng, C., Ravindra, P., 2011. Economic assessment of biodiesel production: comparison of alkali and biocatalyst processes. Renew. Sust. Energ. Rev. 15, 745–751 doi.org/10.1016/j.rser.2010.07.055.

Karmee, S.K., Patria, R.D., Lin, C.S.K., 2015. Techno-economic evaluation of biodiesel production from waste cooking oil—a case study of Hong Kong. Int J. Mol. Sci. 16, 4362–4371. Doi:10.3390/ijms16034362.

Morone, P., Yilan, G., 2020. A paradigm shift in sustainability: from lines to circles. Acta Innov. 5–16 (36), 5 doi.org/10.32933/ActaInnovations.36.1.

Moser, B.R., 2016. Fuel property enhancement of biodiesel fuels from common and alternative feedstock via complementary blending. Renew. Energy 85, 819–825. DOI: 10.1016/j.renene.2015.07.040.

Oni, B.A., Oluwatosin, D., 2020. Emission characteristics and performance of neem seed (Azadirachta indica) and Camelina (Camelina sativa) based biodiesel in diesel engine. Renew. Energy 149, 725–734 doi.org/10.1016/j.renene.2019.12.012.

Oni, B.A., Sanni, S.E., Okoro, E., 2021. E, Performance evaluation of Nannochloropsis oculate carbon nanoparticle blend as fuel in compression ignition engine. Biofuel, Bioprod. Bioref. doi:10.1002./bbb/2335.

Oni, B.A., Sanni, S.E., Ibegbu, A.J., Aduojo, A.A., 2021. Experimental optimization of engine performance of a dual-fuel compression-ignition engine operating on hydrogen-compressed natural gas and Moringa biodiesel. Energy Rep. 7, 607–619 doi.org/10.1016/j.egyr.2021.01.019.

Oni, B.A., Sanni, S.E., Daramola, M., Olawepo, A.V., 2021. Effects of oxy-acetylation on performance, combustion and emission characteristics of Botryococcus braunii microalgae biodiesel-fuelled CI engines 59. Fuel, 120675 doi.org/10.1016/j.fuel.2021.120675.

Oni, B.A., Sanni, S.E., Alaba, P.A., Hessien, M.M., El-Bahy, Z.M., 2021. Investigating the performance of acetylated diethyl ether–Camelina sativa biodiesel as fuel in compression ignition engine Energy. Ecol. Environ. doi.10.1007/s40974-012-00230-5.

Oni, B.A., Sanni, S.E., Orodu, O.D., Ogunkunle, T.F., 2021c. Comparing the effects of Juliflora biodiesel doped with Nano additives on the performance of a compression ignition (CI) engine: Part A. Energy, 122635. https://doi.org/10.1016/j.energy.

Oni, B.A., Sanni, S.E., Ezurike, B.O., Okoro, E.E., 2022. Effect of corrosion rate on preheated Schinzochytrium sp. Microalgae biodiesel on metallic component of a diesel engine. Alex. Eng. J. doi.org/10.1016/j.aej.2022.01.005.

Ors, I., Sarıkoc, S., Atabani, A.E., Unalan, S., Akansu, S.O., 2018. The effects on performance,combustion and emission characteristics of DICI engine fuelled with TiO2 nanoparticles addition in diesel/biodiesel/n-butanol blends. Fuel 234, 177–188 doi.org/10.1016/j.fuel.2018.07.024.

Paramashivaiah, B., Banapurmath, N., Rajashekhar, C., Khandal, S., 2018. Studies on effect of graphene nanoparticles addition in different levels with Simarouba biodiesel and diesel blends on performance, combustion and emission characteristics of CI engine. Arab. J. Sci. Eng. 1–9 doi.org/10.1007/s13369-018-3121-6.

Pinzi, S., Garcia, I.L., Lopez-Gimenez, F.J., Luque de Castro, M.D., Dorado, G., Dorado, M.P., 2009. The ideal vegetable oil-based biodiesel composition: a review of social, economic and technical implications. Energy Fuels 23 (5), 2325–2341 doi.org/10.1021/ef801098a.

Praveen, A., Lakshmi Narayana Rao, G., Balakrishna, B., 2017. Performance and emission characteristics of a diesel engine using Calophyllum inophyllum biodiesel blends with $TiO_2$ nanoadditives and EGR. Egypt J. Pet. 11/10/2017. doi.org/10.1016/j.ejpe.2017.10.008.

Ruan, B., Jacobi, A.M., 2012. Ultrasonication effects on thermal and rheological properties of carbon nanotube suspensions. Nanoscale Res. Lett. 7 (1), 127. DOI: 10.1186/1556-276X-7-127.

Sakai, T., Kawashima, A., Koshikawa, T., 2009. Economic assessment of batch biodiesel production processes using homogeneous and heterogeneous alkali catalysts. Bioresour. Technol. 100, 3268–3276 doi.org/10.1016/j.biortech.2009.02.010.

Simsek, S., Uslu, S., 2020. Comparative evaluation of the influence of waste vegetable oil and waste animal oil-based biodiesel on diesel engine performance and emissions. Fuel 280, 118613 doi.org/10.1016/j.fuel.2020.118613.
Soudagar, M.E.M., Nik-Ghazali, N.-N., Abul Kalam, M., Badruddin, I.A., Banapurmath, N.R., Akram, N., 2018. The effect of nano-additives in diesel-biodiesel fuel blends: a comprehensive review on stability, engine performance and emission characteristics. Energy Convers. Manag 178, 146–177 doi.org/10.1016/j.enconman.2018.10.019.
Yesilyurt, M.K., Cesur, C., 2017. Biodiesel synthesis from Styrax officinalis L. seed oil as a novel and potential non-edible feedstock: a parametric optimization study through the Taguchi technique. Fuel 207, 690–701 doi.org/10.1016/j.fuel.2020.117025.